Dynamics and Structural Details of Amorphous Phases of Ice Determined by Incoherent Inelastic Neutron Scattering

D. D. Klug, C. A. Tulk, and E. C. Svensson
Steacie Institute for Molecular Sciences, National Research Council of Canada, Ottawa, Ontario, Canada K1A 0R6

C.-K. Loong
Intense Pulsed Neutron Source Division, Argonne National Laboratory, Argonne, Illinois 60439
(Received 16 February 1999)

Incoherent-inelastic neutron scattering data are obtained over the energy range of lattice and internal vibrations of water molecules in phases of ice prepared by pressure-induced amorphization (high-density amorphous ice, hda), by thermal annealing of hda (low-density amorphous ice, lda), and by rapidly cooling water, as well as in ice Ih and Ic. Hydrogen bonding interactions in lda differ significantly from those in the glass obtained by rapid quenching, which has hydrogen-bond interactions characteristic of highly supercooled water. Hydrogen-bond interactions in hda are weaker than in the low-density phases.

PACS numbers: 61.43.Er, 61.12.–q, 61.20.Ne, 61.43.Fs

The structure of the amorphous solid phases of ice has been an important area of study since the discovery by Mishima *et al.* [1] of high-density amorphous ice (hda), prepared by pressurizing ice Ih to 12 GPa at 77 K. The relationship of the structure of hda to that of a postulated high-density form of liquid water is currently of particular interest since there is the possibility that water may have at least two coexisting structures at low temperatures and there may be a second critical point at low temperatures [2]. The long-standing problem to define the relation between liquid water at room temperature and the glassy solid prepared by rapid cooling [3] is also of high current interest.

Both neutron and x-ray diffraction have been employed to obtain structural information on the amorphous phases of ice in order to compare their structures to those of the crystalline phases of ice and of liquid water [4–6]. There have been several suggestions regarding the structures of the amorphous phases, such as the proposal that the high-density form prepared by pressure-induced amorphization is similar to that of a quenched high-density liquid [1]. This hypothesis supports a suggestion that the mechanism for the process of the pressure-induced amorphization of ice Ih is describable as a thermodynamic melting process [1,2]. Conventional diffraction methods, however, have not been sensitive enough to characterize differences between the low-density amorphous phases prepared by different techniques [6] and therefore may not be able to supply definitive information to characterize the relationship between hda and high-density quenched water. Infrared and Raman vibrational spectroscopy are extremely sensitive to the local environment of water molecules in the amorphous phases since there are changes in frequency with hydrogen bond O-H $\cdots$ O lengths of $\sim$1000 cm^{-1}/Å [7,8].

The purpose of this Letter is to demonstrate that incoherent inelastic neutron scattering (IINS) can reveal details of the dynamics of crystalline and amorphous phases of ice and also reflect their subtle structural differences, via the measured density of states. This reflects the fact that IINS from librational and intramolecular vibrations of water molecules is extremely sensitive to the local environments of water molecules in the amorphous and crystalline ices. Moreover, IINS is not restricted by selection rules; therefore, all vibrational modes contribute to the observed spectra. Consequently, a more precise comparison of the structural details of the amorphous phases can in principle be made.

hda was prepared by pressurizing ice Ih to 14 GPa at 77 K. They were contained in liquid nitrogen and mounted in a cell of planar geometry (75 by 100 mm) with a thickness of about 1–2 mm that was then maintained at 15 K for the neutron scattering measurements. After data were collected on this sample, it was annealed at 120 K for 10 min to transform it to low-density amorphous ice (lda) and cooled back to 15 K for measurements. The sample was then annealed at 150 K to first form ice Ic and then at 240 K to produce ice Ih. Hyperquenched water (hqw) was prepared by rapid cooling (10^6 K/s) of 3 micron diameter water droplets by transporting the droplets through a glass tube in nitrogen carrier gas and splat cooling them onto a 78 K cold plate in a vacuum chamber using a method similar to that described previously [9]. The rapidly cooled water was verified to be amorphous by x-ray diffraction.

The neutron scattering measurements were performed using the High-Resolution Medium Energy Chopper Spectrometer [10–12] at the Intense Pulsed Neutron Source of Argonne National Laboratory. Incident neutron energies (E_0) of 300 and 600 meV were used so as to cover the frequency regions of both the librational and internal stretching vibrations with good resolution. The energy resolution $\Delta E/E_0$ (ΔE = full width at half maximum) was approximately 3% at the upper end of the neutron-energy-loss spectrum. The low scattering angles ($<20°$) result in a relatively low wave-vector transfer Q ($\sim$3 and $\sim$8 Å^{-1} at

 0031-9007/99/83(13)/2584(4)$15.00

energy transfers of 80 and 450 meV, respectively) for the high incident energies E_0 used in this study. The Doppler broadening of the vibrational peaks is therefore kept reasonably low.

The scattering functions for four phases studied at 15 K are shown in Figs. 1 and 2. The band observed in the region from 50 to 130 meV is due to the coupled librational modes determined primarily by the short-range hydrogen bonding interactions that restrict rotation of the water molecules. The librational modes are well separated from the low-frequency lattice translational vibrations. The broad bandwidth results from intermolecular coupling in the lattice. In all phases the scattering function has a similar shape, namely, a sharp leading edge at low energy followed by a distinct maximum and a broad featureless shoulder at the high-energy side of the band. The widths of the bands, as measured at the half height are 47.8, 50.8, 50.1, and 51.6 meV for hda, lda, hqw, and ice Ih, respectively. The hda phase has the lowest average energy and the broad maximum occurs at 71 meV; lda and ice Ih have very similar spectra with the broad maxima at 80 meV and their distributions have highest average energy. hqw has a spectrum that is clearly different from that of the other phases; it is intermediate in energy between hda and both lda and ice Ih and the broad maximum occurs at 75 meV. The spectrum of ice Ic is identical to that for ice Ih and is therefore not shown. The onset frequencies for the hda, ice Ih, and lda phases are in good agreement with earlier measurements using reactor and pulsed neutron sources [13,14]. Results for the other regions (160–240 meV, 350–500 meV) where bands are observed in the present study have not been previously reported for these ice phases except for ice Ih [10,14] and for hda in a study [15] that has just appeared. The half-widths of the peaks in this region for hda, lda, hqw, and ice Ih are 16, 35, 26, and 37 meV, respectively. In the region 350–500 meV (Fig. 2) the peaks corresponding to intramolecular stretching modes have energies that are in the reverse order to that found in the low energy librational range (see Fig. 1). The peak energies for hda, lda, hqw, and ice Ih are 426, 412, 420, and 415 meV, respectively. In this region, the onset energies are very similar in all phases, but hda has a distinctly larger contribution at the highest energy edge of this band and its leading-edge and peak energies are about 15 meV higher than those for lda, and ice Ih and lda have similar peak frequencies. hqw liquid has a peak frequency that is intermediate between the lda and hda phases. The uncertainty of the data in Figs. 1 and 2 is indicated by the size of the circles, except for the much smaller hqw sample, where the uncertainty is reflected by the scatter of the points seen in the wings. The differences in the high-energy region are more subtle than in the 50–160 meV region. Raman data of uncoupled OH or OD vibrations in dilute solutions of H_2O in D_2O or D_2O in H_2O, respectively [16], can also almost entirely eliminate the complication of selection rules since these techniques sample the O-H or O-D vibration for the isolated HOD molecule in the lattice. The Raman-active mode is narrow due to the lack of the intermolecular or intramolecular coupling. The energy for the O-H Raman active mode [9,16] at 10 K in hqw (409.4 meV) is between that of hda (414.3 meV) and lda (406.7 meV) and this supports our conclusions. These results clearly distinguish between the amorphous ice polymorphs and show that the spectra of lda and ice Ih are quite similar.

The vibrational energies for the intramolecular bond stretching vibrations are known to have an energy dependence [7] on the hydrogen-bond length O-H $\cdots$ O in crystalline phases of ice of $\sim$1000 cm^{-1}/Å or 124 meV/Å. The observed differences in the spectra among the amorphous phases and the similarities of the IINS spectra of lda and ice Ih can be interpreted in terms of the distribution of

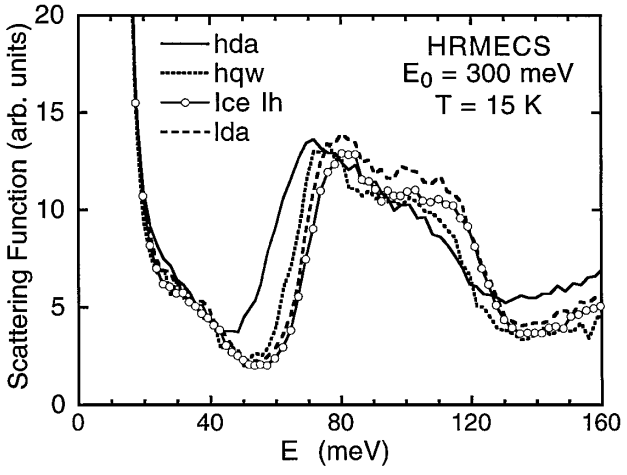

FIG. 1. The neutron scattering function for the librational modes of amorphous (lda and hda) and crystalline phases of ice (Ih) and hyperquenched water (hqw). The uncertainty of the data points is described in the text.

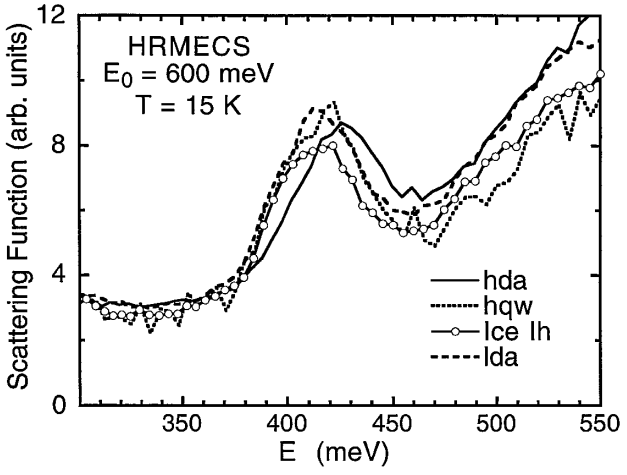

FIG. 2. The neutron scattering function for the O-H stretching modes for amorphous (lda and hda) and crystalline (Ih) phases of ice and hyperquenched water (hqw). The uncertainty of the data points is described in the text.

the short-range hydrogen-bond interactions, i.e., therefore can be related to the average hydrogen bonded O-H $\cdots$ O length distributions. Water is $\sim$10% denser than ice Ih at ambient pressure, reflecting the higher oxygen coordination number of 4.4 (the average number of first neighbor water molecules around a central molecule [17]). The higher density of water is accompanied by a longer average O-H $\cdots$ O bond length of 2.82 Å compared to 2.76 Å in ice Ih. hda has a density of 1.17 ± 0.02 g/cm^3 at ambient pressure and 77 K, and the densities of lda and hqw are 0.94 ± 0.02 and 0.95 ± 0.02 g cm^{-3}, respectively [18,19]. It is likely that hda has a higher nearest neighbor oxygen coordination number than ice Ih or water since the average hydrogen bond lengths are known to be longer in hda than in liquid water or ice Ih [16]. This structural information is reflected in the vibrational density of states obtained from IINS.

For the broad peak in the range 50–150 meV, the mean or peak energies and onset energies for hda are significantly lower than those of hqw, lda, or ice Ih. The vibrations in this energy range result from hindered rotations (librational modes) of water molecules. The observed mean energy and bandwidth provide a measure of the strength of intermolecular coupling. The approximately 10 meV lower onset energy and mean energy of the hda band compared with the other phases, as well as the lower mean energies of the broad shoulders, are a result of weaker intermolecular interactions that restrict librational modes less in hda than in hqw, lda, and ice Ih. The distributions for lda and ice Ih are similar, while the hqw energies are intermediate between hda and the lda and Ih phases. The opposite trend is observed in the range 350–500 meV, where the peak and mean energies for hda are approximately 10 meV higher than those of lda and ice Ih. This opposite trend in energy was observed in Raman data and both are entirely consistent with the dynamic response of intramolecular and intermolecular interactions in a hydrogen-bonded system. A weaker hydrogen-bond interaction would yield a lower energy for librational modes of water molecules in the solid. This weaker interaction would also be reflected in intramolecular vibrational mode energies closer to those of an isolated molecule and, in the case of O-H stretch vibrations, would yield higher energies. The peak widths and peak energies are a direct mapping of the hydrogen bond interactions that perturb the intramolecular vibrations. A stronger intermolecular hydrogen bond will yield lower energies due to an effective weakening of the directly bonded O-H interaction. This trend is well documented, and correlations between the energy and the O-H $\cdots$ O distances are known [6]. The coupled intramolecular and intermolecular vibrations of water molecules also give rise to the broadening of the O-H stretch vibrational band (Fig. 2). The observed width of the band ($\sim$50 meV for all phases studied) reflects the large range of vibrational energies that result from molecules located in different hydrogen-bonded environments in addition to the coupling between individual modes. These contributions cannot be separated in the IINS experiments; instead, the observed peak should be regarded as a density of stretch vibrational states. The Raman technique measures the vibrational modes at $Q = 0$, and Raman data for the uncoupled O-H or O-D modes from dilute solution measurements provides a measure of the distribution of local interactions. This information can be used together with the IINS data to estimate the contributions to the bandwidth arising from intermolecular and intramolecular coupling. The bandwidth of the localized O-H vibrations in the Raman spectra varies from $\sim$6 meV in ice Ih to $\sim$13 meV in hda. These values, amounting to 13% and 35% of the total bandwidth in these two phases, respectively, indicate that the major contribution to the bandwidths is due to intermolecular and intramolecular coupling.

Several details of the structural relationship between the amorphous phases of ice and liquid water can be obtained from a comparison with previous measurements [11,12]. A plot of the peak energies versus temperature for liquid water and hqw (Fig. 3) support the hypothesis that there is continuity of structure between the high temperature liquid water structure and that of hqw. hqw has a peak energy of about 420 meV at 15 K as compared to 434 meV for liquid water at 313 K. The half-width of the peak is 43 meV for hqw at 15 K compared to 54 meV for supercooled water [10] at 258 K. The hyperquenching process cools liquid water rapidly enough to avoid crystallization and "captures" the liquid structure at a low temperature. The temperature at which water is immobilized upon quenching, defined as the fictive temperature, has been shown to be

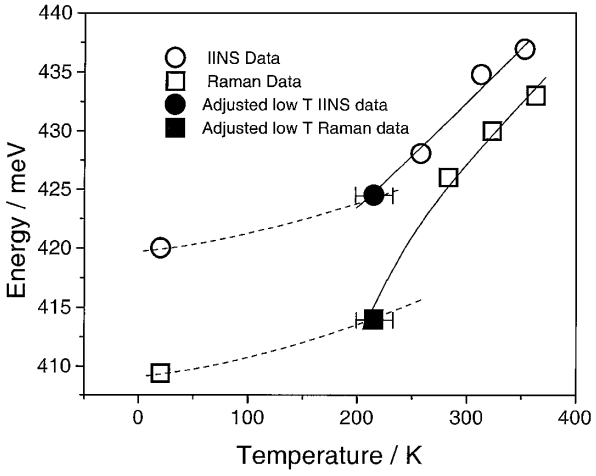

FIG. 3. Temperature dependence of peak energies of liquid water in the O-H stretching mode region for supercooled liquid water, and hqw from Raman spectroscopy and IINS. The dashed lines showing corrections for anharmonic effects connect the results obtained at 15 K with these results corrected for anharmonic effects to the fictive temperature of the hqw. The range of fictive temperatures is shown by the horizontal bars (for details see text).

between 200 and 230 K [20]. The energy distributions for hqw shown in Figs. 1 and 2 reflect the structure of water *at the temperature where it undergoes the transformation to a glassy solid* with exclusion of anharmonic effects that arise from thermal expansion and volume independent anharmonic contributions upon cooling from the fictive temperature to 15 K. The liquid structure for which the spectra are reported in both the present IINS data and the recent Raman data [9] therefore reflects the structure of water at a temperature in the range 200 to 230 K. Both spectra also include the reduction of the anharmonic contributions as a result of lowering the temperature to 15 K. An estimate of these contributions is available from measurements on the temperature dependence of the spectra of ice Ih and vapor-deposited amorphous ice [21]. Extrapolation of the data for the energy dependence of the uncoupled O-H oscillator in these materials [21] indicates that the anharmonic contribution to the energy shifts is $\sim$35 cm^{-1} or $\sim$4.5 meV in cooling from 200 to 15 K for both materials. A reasonable estimate of the peak frequencies for the internal mode spectra of the quenched liquid at the fictive temperature (200–230 K) can be made by adding the estimated anharmonic contribution to the frequencies obtained at 15 K yielding the values shown by the filled symbols. The dashed lines in Fig. 3 show the effect of the anharmonic corrections obtained from Ref. [21].

The slight nonlinear extrapolation for the Raman data [9,22] as compared to the IINS data may be due to selection rule effects or to a possible overestimate of the fictive temperature [20]. The smooth decline in peak energy with decreasing temperature that is seen in Fig. 3 gives no indication of the presence of the anomalous behavior that would be expected to be associated with proposed critical behavior [3] at $\sim$230 K. It appears therefore from the present study that there is a continuity of state between liquid water above its melting temperature, and hqw.

The IINS spectra for the phases of ice reported here demonstrate that there are substantial structural differences between these phases of ice that are not revealed by existing elastic scattering data. The radial distribution function for the low-density amorphous phase prepared by vapor deposition has been reported [6] to be indistinguishable from that for hqw. Raman data support this finding [9] but show that there are distinct differences between hqw and lda prepared by annealing hda.

It is clear that the lda phase of ice is more closely related to the ice Ih structure than to hqw. It has been shown that hda is also more closely related to crystalline ice than to dense liquid water in recent lattice dynamics calculations [23] and by molecular dynamics simulations [24] of the amorphization of ice Ih.

In summary, IINS data provide a direct comparison of high- (hda) and low-density amorphous ice (lda), ice Ic, ice Ih, and hqw in the energy regions of the librational and internal vibrational modes of the water molecules. The hqw has stronger hydrogen-bond interactions and therefore a shorter average hydrogen-bond length than hda. In fact, hda is characterized by weaker hydrogen bonds than occur in lda, hqw, or ice Ih and Ic. hqw has weaker average hydrogen-bond interactions than those observed in lda and ice Ih or Ic. The densities of vibrational states for lda and ice Ih are very similar and clearly different from that of hqw. The peak energy, corrected for effects of anharmonicity, indicates a direct connection between the liquid and glassy phase of water.

The work performed at Argonne National Laboratory is supported by the U.S. DOE-BES under Contract No. W-31-109-ENG-38. We thank D. Yokum for his assistance with the IINS experiments.

[1] O. Mishima, L. D. Calvert, and E. Whalley, Nature (London) **310**, 393 (1984).
[2] O. Mishima and E. H. Stanley, Nature (London) **392**, 164 (1998).
[3] C. A. Angell, Nature (London) **331**, 206 (1988).
[4] L. Bosio, G. P. Johari, and J. Teixeira, Phys. Rev. Lett. **56**, 460 (1986).
[5] M. A. Floriano *et al.*, Phys. Rev. Lett. **57**, 3062 (1986).
[6] M. C. Bellissent-Funel *et al.*, J. Chem. Phys. **97**, 1282 (1992).
[7] D. D. Klug and E. Whalley, J. Chem. Phys. **81**, 1220 (1984).
[8] E. Whalley, in *The Hydrogen Bond in Ice*, edited by P. Schuster, G. Zundel, and C. Sandorfy (North-Holland, Amsterdam, 1976), Vol. III, p. 1427.
[9] C. A. Tulk *et al.*, J. Chem. Phys. **109**, 8478 (1998).
[10] K. Toukan *et al.*, Phys. Rev. A **37**, 2580 (1988).
[11] S.-H. Chen *et al.*, Phys. Rev. Lett. **53**, 1360 (1984).
[12] C. Andreani *et al.*, J. Chem. Phys. **83**, 750 (1985).
[13] D. D. Klug *et al.*, Phys. Rev. B **44**, 841 (1991).
[14] J. C. Li, J. Chem. Phys. **105**, 6733 (1996).
[15] A. I. Kolesnikov *et al.*, Phys. Rev. B **59**, 3569 (1999).
[16] D. D. Klug, O. Mishima, and E. Whalley, J. Chem. Phys. **86**, 5323 (1987).
[17] A. H. Narten and H. A. Levy, Science **165**, 447 (1969).
[18] G. Fleissner, A. Hallbrucker, and E. Mayer, J. Phys. Chem. **102**, 6239 (1998).
[19] O. Mishima, L. D. Calvert, and E. Whalley, Nature (London) **314**, 76 (1985).
[20] W. Hage, A. Hallbrucker, and E. Mayer, J. Phys. Chem. **96**, 6488 (1992).
[21] M. G. Sceats and S. A. Rice, in *Water: A Comprehensive Treatise*, edited by F. Franks (Plenum Press, New York, 1984), Vol. 7, p. 83.
[22] J. R. Scherer, M. K. Go, and S. Kint, J. Phys. Chem. **78**, 1304 (1974).
[23] J. S. Tse and D. D. Klug *et al.* (to be published).
[24] J. S. Tse, J. Chem. Phys. **96**, 5482 (1992).